Chemistry & Biology, Vol. 12, 1349–1357, December, 2005, ©2005 Elsevier Ltd All rights reserved. DOI 10.1016/j.chembiol.2005.10.005

De Novo Design of α-Amylase Inhibitor: A Small Linear Mimetic of Macromolecular Proteinaceous Ligands

Lucie Dolečková-Marešová,[1] Manfred Pavlík,[1] Martin Horn,[1] and Michael Mareš[1,*]
[1] Institute of Organic Chemistry and Biochemistry
Academy of Sciences of The Czech Republic
Flemingovo nam. 2
16610 Praha
Czech Republic

Summary

We report a low molecular weight inhibitor of α-amylases based on a linear peptidic scaffold designed de novo through the use of combinatorial chemistry. The inhibitory motif denoted PAMI (*p*eptide *am*ylase *i*nhibitor) was selected by using L-peptide libraries and was fine-tuned by the introduction of unnatural modifications. PAMI specifically inhibits glycoside hydrolases of family 13. Its interaction with porcine pancreatic α-amylase was characterized by inhibition kinetics, fluorescence competition assays with natural α-amylase inhibitors, and isothermal titration calorimetry. We demonstrate that the critical amino acid residues in PAMI are shared with those in the macromolecular proteinaceous inhibitors that, however, bind to α-amylases through a spatially scattered set of intermolecular contacts. Thus, natural molecular evolution as well as combinatorial evolution selected the same α-amylase binding determinants for completely different spatial frameworks.

Introduction

α-amylases (α-1,4-glucan-4-glucanohydrolases) are a group of glycoside hydrolases widely distributed in microorganisms, plants, and animal tissues. They catalyze the hydrolysis of the α-(1,4) glycosidic linkage found in starch components and other related polysaccharides. α-amylases are among the oldest known enzymes; however, detailed information about their structure and inhibition started to come to light only in the '90s as they became a target for regulation of important physiological processes. Currently, there are two major applications of α-amylase inhibitors. Orally given α-amylase inhibitors, such as the antidiabetic drug acarbose, suppress postprandial glucose levels in diabetic patients (for a review, see [1]). The second promising field is the potential use of α-amylase inhibitors in transgenic crops to suppress the development of insect pests through the impairment of their amylolytic digestion (for a review, see [2]).

The natural inhibitors of α-amylases comprise oligosaccharide inhibitors of the trestatin family from *Streptomyces* that contain the acarviosine moiety (e.g., acarbose) and proteinaceous inhibitors isolated from microbial sources and plant tissues [3, 4]. The plant inhibitors have two main functions: they regulate endogenous α-amylase activity in seeds, or they act as defensive proteins directed against exogenous digestive α-amylases of insect herbivores [2]. The α-amylase inhibitors of protein character compose seven structurally different protein families, and, for five of them, X-ray structures of the complexes with α-amylase were determined thus far [5–9]. These spatial models revealed that the structural mechanism of inhibitory complex formation with the target enzyme evolved in a specific way for each family of the inhibitors. As the proteinaceous α-amylase inhibitors are strong ligands (with inhibition constants mostly in nanomolar range), their binding is generally established through an extended set of intermolecular contacts with several segments of the polypeptide chain involved in the binding. Due to the complicated architecture, the rational design of small inhibitory mimetics of these macromolecular ligands is a difficult task. However, this problem can be efficiently approached through the application of combinatorial technologies to generate vast molecular diversities and select de novo ligand structures. The first attempts to use a combinatorial repertoire for the development of α-amylase inhibitors were done recently with the phage display method, but this effort led to novel ligands having the macromolecular protein scaffold [10, 11]. Interestingly, the powerful approach of combinatorial chemistry that is very successful in the development of novel low-molecular weight therapeutics has not been applied for this purpose thus far.

To our knowledge, we report the first low-molecular weight inhibitory motif for α-amylases designed de novo through the use of combinatorial chemistry. The structural requirements and interaction mode of the discovered inhibitory ligands were characterized in detail by kinetic, fluorescence, and calorimetric methods. This analysis revealed that the small peptidic recognition motif represents a molecular mimicry of the macromolecular α-amylase inhibitors, as it effectively arranges the analogous structural determinants in a simple, linear scaffold. Finally, unnatural derivatives of the lead peptide inhibitor were developed as more potent α-amylase inhibitors than the antidiabetic drug acarbose [3] or small α-amylase ligands constructed by rational design [12, 13].

Results

De Novo Design of the α-Amylase Inhibitory Motif

Porcine pancreatic α-amylase (PPA) was used as a target enzyme for the screening of inhibitory activity of combinatorial L-peptide libraries by using a standard assay with chromogenic substrate Remazol Brilliant Blue-dyed starch (RBB-Starch). In the first step, we prepared 400 sublibraries with 2 fixed amino acids at the N terminus in the format Ac-B_1B_2XXXX-NH_2 (B, defined position; X, randomized position). Screening of sublibraries for PPA inhibition guaranteed the selection of the most effective inhibitory mixture, Ac-HWXXXX-NH_2 (Figure 1). In the next step, preference for the third position was studied with a library of second generation

*Correspondence: mares@uochb.cas.cz

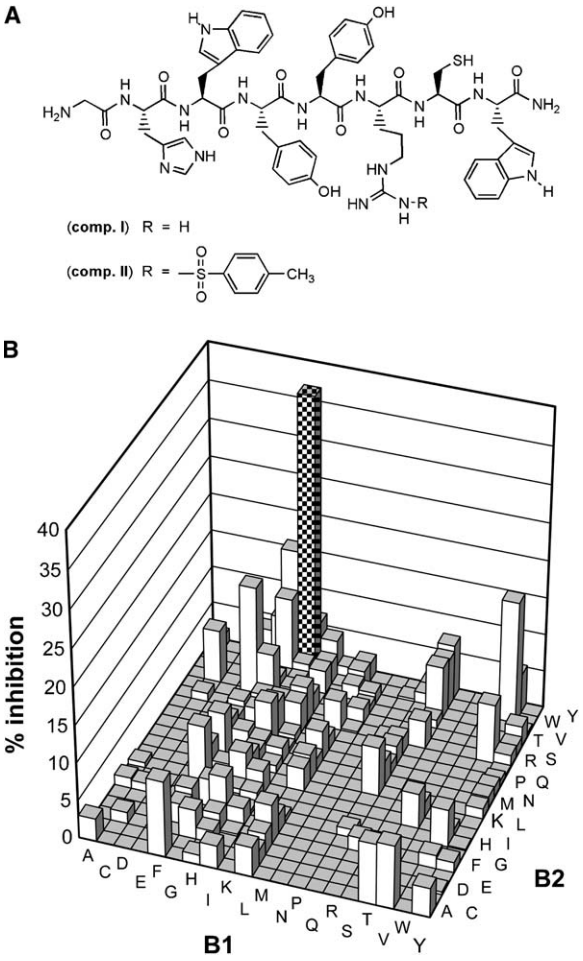

Figure 1. Combinatorial Design of the α-Amylase Inhibitory Motif PAMI

(A) Structure of the lead peptide molecule GHWYYRCW-NH_2 selected through the complete procedure (comp. I) and its unnatural tosyl derivative with improved inhibitory potency (comp. II).

(B) The first step in the selection procedure: screening of 400 peptide sublibraries of the Ac-B_1B_2XXXX-NH_2 structure for inhibition of PPA activity. The most inhibitory sublibrary, Ac-HWXXXX-NH_2, is highlighted. "B" indicates the defined position with 1 of 20 proteinogenic L-amino acids, and "X" indicates the random position with an equimolar mixture of 20 proteinogenic L-amino acids; values are expressed as the percentage of activity relative to the uninhibited control. PPA (10 pM) was assayed at pH 6.9 with the chromogenic substrate Remazol Brilliant Blue-dyed starch (0.3%, w/v) and 50 μg/ml peptides.

Ac-HWB_3XXX-NH_2 composed of 20 individual sublibraries, leading to the most efficient sublibrary, Ac-HWYXXX-NH_2 (Table 1). Analogously, an iterative selection process was performed to sequentially define the remaining X positions in the C-terminal direction with libraries Ac-HWYB_4XX-NH_2 to Ac-HWYYRB_6-NH_2. This procedure gradually improved the inhibitory potential of the derived combinatorial ligands and identified the hexapeptide core with sequence HWYYRC, which displayed an IC_{50} value in the micromolar range (Table 1). The inhibition potency was further improved by extending the core in the N- and C-terminal directions with libraries Ac-HWYYRCB_7-NH_2 and Ac-B_8HWYYRCW-NH_2. The delineated sequence GHWYYRCW represents the octapeptide motif for α-amylase inhibition further denoted as PAMI (*p*eptide *am*ylase *i*nhibitor) (Figure 1). In Table 1, we also present results on an alternative branch of the iterative procedure split in the B_3 position for which Trp residue was approaching the efficiency of the most inhibitory Tyr residue. Interestingly, this selection process resulted in identification of the hexapeptide sequence HWWRCW that closely resembles the sequence obtained for the Tyr branch (HWYYRC); however, this sequence is frame shifted by one residue. It appears that the structural block of WYYR might be functionally equivalent to the WWR block concerning its contribution to the binding.

Table 1. Iterative Scheme to Define the α-Amylase Inhibitory Motif PAMI

Library	Sublibrary	IC_{50} (μM)[a]
Ac-B_1B_2XXXX-NH_2	Ac-HWXXXX-NH_2	~200
Ac-HWB_3XXX-NH_2	Ac-HWYXXX-NH_2	107.5
	Ac-HWWXXX-NH_2	95.3
Y_3 Iteration		
Ac-HWYB_4XX-NH_2	Ac-HWYYXX-NH_2	35.3
Ac-HWYYB_5X-NH_2	Ac-HWYYRX-NH_2	27.4
Ac-HWYYRB_6-NH_2	Ac-HWYYRW-NH_2	20.5
	Ac-HWYYRC-NH_2	16.2
Ac-HWYYRCB_7-NH_2	Ac-HWYYRCL-NH_2	12.2
	Ac-HWYYRCR-NH_2	10.7
	Ac-HWYYRCY-NH_2	10.1
	Ac-HWYYRCW-NH_2	6.3
Ac-B_8HWYYRCW-NH_2	Ac-WHWYYRCW-NH_2	4.8
	Ac-YHWYYRCW-NH_2	4.5
	Ac-GHWYYRCW-NH_2	4.1
W_3 Iteration		
Ac-HWWB_4XX-NH_2	Ac-HWWRXX-NH_2	33.4
Ac-HWWRB_5X-NH_2	Ac-HWWRCX-NH_2	28.5
Ac-HWWRCB_6-NH_2	Ac-HWWRCW-NH_2	25.3
	Ac-HWWRCR-NH_2	16.4

The sublibraries most inhibitory against PPA are listed with the IC_{50} values determined. "B" indicates the defined position with 1 of 20 proteinogenic L-amino acids, and "X" indicates the random position with an equimolar mixture of 20 proteinogenic L-amino acids. The Y_3 and W_3 iterations represent two parallel branches of the iterative scheme derived from the Ac-HWB_3XXX-NH_2 library with two potent inhibitory sublibraries (B_3 = Y or W).

[a] The peptide libraries were screened for inhibition of PPA activity in an assay with 10 pM enzyme and 0.3% (w/v) Remazol Brilliant Blue-dyed starch as substrate at pH 6.9.

Unnatural Modification of the Inhibitory Motif

To further improve its efficiency, the PAMI motif was modified by specific unnatural substitutions and by conformational changes of its scaffold. A panel of the derivatives and their inhibitory potency are listed in Table 2. First, the position of structurally distinct determinants of Arg_5 and Cys_6 was studied. The side chain of arginine was modified by Pmc or a tosyl group, both containing an aromatic moiety with a sulfonyl group, which resulted in the improvement of the inhibition by an order of magnitude. On the other hand, the substitution of arginine with citrulline totally abolished the inhibition, suggesting that the guanidino group cannot be substituted by its isosteric urea homolog. Modification of the cysteine side chain with an apolar t-butyl group or a polycyclic aromate fluorescein did not dramatically change the inhibition. However, an introduction of the polar group of

Table 2. Screening of Derivatives of the α-Amylase Inhibitory Motif PAMI for Inhibition of PPA Activity

Structure[a]		IC_{50} (μM)[b,c]	
		Ac-/Alkyl-	NH_2-
Arg and Cys substitution			
HWYYR(Tos) C		1.7 ± 0.3	
GHWYYR(Tos)CW	comp. II	2.6 ± 1.2	0.5 ± 0.2
GHWYYR(Tos)C(tBu)W			1.9 ± 0.4
HWYYCitrC		n.s.i.	
GHWYYR(Pmc)CW		0.9 ± 0.3	
GHWYYR(Pmc)C(Acm)W		5.1 ± 1.1	
GHWYYRC(Acm)W		171.2 ± 23.5	
GHWYYRC(tBu)W		6.1 ± 2.0	6.8 ± 1.9
GHWYYRC(Flu)W	comp. IV	7.6 ± 1.4	
Tyr-Tyr substitution			
GHWZ(Tpc)Z(Tpc)RCW		125.1 ± 17.3	
GHWZ(Tpg)Z(Tpg)RCW		173.9 ± 19.1	
GHWF(pCl)F(pCl)RCW		178.3 ± 21.8	
GHWA(cHx)A(cHx)RCW		115.2 ± 18.4	
GHWWRCW		12.4 ± 2.2	
Terminus modification			
GHWYYRCW-COOH		4.2 ± 0.4	4.6 ± 1.1
GHWYYRCW	comp. I	4.1 ± 0.9	5.1 ± 0.9
Flu-GHWYYRC(tBu)W	comp. III	19.6 ± 3.1	
Lac(C_8)-GHWYYRCW		n.s.i.	
Scaffold modification			
GHWYYRCW-γAbu-GHWYYRCW		0.5 ± 0.2	1.6 ± 0.3
GHWYYRCW		8.3 ± 1.5	
GHWYYRCW			
CGHWYYRC(tBu)WC			n.s.i.
D-amino acid substitution			
ghwyyrcw			171.8 ± 8.5

The modified peptides (0–250 μM) were assayed with 10 pM enzyme and 0.3% (w/v) RBB-Starch as substrate at pH 6.9. The compounds were synthesized in the form of peptidyl amides containing a free (NH_2-) or acetylated (Ac-) N terminus, or they were modified at the N terminus by attachment of a specified group. The compounds referred to in the text are indicated (comp. I–IV).

[a] R(Tos), tosyl-arginine; C(tBu), t-butyl-cysteine; R(Pmc), 2,2,5,7,8-pentamethyl-chromane-6-sulfonyl-arginine; Citr, citruline; C(Acm), acetamidomethyl-cysteine; Z(Tpc), 4-aminotetrahydropyran-carboxylic acid; Z(Tpg), tetrahydropyran-4-yl-glycine; F(pCl), p-chloro-phenylalanine; A(cHx), cyklohexylalanine; C(Flu), fluorescein- acetamido-cysteine; Flu, fluoresceinyl; Lac(C_8), mono(lactosylamido)suberyl; γAbu, 4-aminobutyric acid; Ac, acetyl.

[b] n.s.i., no significant inhibition with 250 μM peptide.

[c] ±SE of the mean of triplicates is indicated.

Acm resulted in about a 40-fold loss of inhibition. Second, the aromatic cluster of two tyrosine residues was replaced by unnatural cyclic blocs, which significantly decreased the inhibitory effect. This points to the importance of the arrangement of aromatic residues in the PAMI motif. Third, the charge at the N and C termini of PAMI had no significant effect on inhibition, similar to what occurs with bulky group attachment to the N terminus. Interestingly, PAMI was completely inactivated when coupled at the N terminus to a disaccharide unit through an aliphatic linker. Fourth, the PAMI motif composed of L-amino acids was globally converted to the D-peptide conformation. It resulted in significantly decreased, but not eliminated, inhibition, which implicates the flexibility of side chains in partially compensating for the switch in conformation. The cyclization of peptidic structure had a more dramatic effect, and it completely inactivated the PAMI inhibitor. On the contrary, the dimerization of the PAMI motif did not negatively influence its inhibitory properties, as shown by clustering two peptides in a linear arrangement (with a γAbu linker) or via a disulfide bond formed between Cys residues of the motif. These results suggest that the unconstrained conformation of the linear PAMI motif is essential for its efficient binding to α-amylase.

Inhibitory Specificity

The PAMI motif was discovered by using the selection procedure with PPA as a target. Its inhibitory specificity was investigated by using glycoside hydrolases of different substrate specificities covering α-amylases and α-glucosidases of mammalian, insect, fungal, and bacterial origin, as well as other selected α- and β-glycosidases functioning in an exo or endo mode of action (Table 3). The analysis showed that all α-amylases and some of the α-glucosidases tested were sensitive to inhibition. The explanation for this pattern came through classification of the screened enzymes according to membership to different structural families of glycoside hydrolases: all sensitive enzymes belong to family 13, while insensitive enzymes belong to the other seven families tested. We do not exclude the possibility that PAMI may exert inhibition toward an additional family among a vast number of glycoside hydrolase families not included in the screening (see the CAZy database, [14]). In summary, the PAMI motif is probably a family-selective inhibitor that can best recognize the common structural features in the binding clefts of α-amylases and α-glucosidases of family 13. Our screening also shows that various PAMI derivatives differ in their IC_{50}s when tested with different sensitive enzymes (data not shown).

Table 3. Screening of the PAMI Derivative Ac-GHWYYRCW for Inhibition of Activity of Model Glycoside Hydrolases

Enzyme	Origin	IC_{50} (μM)[a]	GH Class
α-amylase	porcine pancreas	4.1 ± 0.9	13
	human saliva	3.2 ± 0.2	13
	Tenebrio molitor	1.1 ± 0.1	13
	Aspergillus oryzae	1.7 ± 0.2	13
	Bacillus amyloliquefaciens	3.1 ± 0.4	13
	Bacillus licheniformis	2.2 ± 0.1	13
	Bacillus subtilis	8.3 ± 0.4	13
α-glucosidase	*Bacillus stearothermophilus*	19.2 ± 0.9	13
	Saccharomyces cerevisiae	2.0 ± 0.3	13
	Schizosaccharomyces pombe	n.s.i.	31
	porcine liver	n.s.i.	31
	porcine intestine	n.s.i.	31
β-glucosidase	sweet almonds	n.s.i.	1
β-galactosidase	*Escherichia coli*	>250	2
cellulase	*Trichoderma viride*	n.s.i.	7
β-amylase	sweet potato	n.s.i.	14
chitinase	*Streptomyces griseus*	>250	18
α-mannosidase	almonds	n.s.i.	38

The structural class of glycoside hydrolases tested is indicated (GH class) according to the CAZy database [14]. n.s.i., no significant inhibition with 250 μM peptide. ±SE of the mean of triplicates is indicated.

[a] For details on particular activity assays, see Experimental Procedures.

Type of Inhibition

A kinetic analysis was performed to determine the inhibition type of PAMI. The hydrolysis of substrate p-nitrophenyl-α-D-maltoheptaoside-4,6-O-ethylidene by PPA follows standard Michaelis-Menten kinetics with a K_M = 85 μM and a k_{cat} of 226 s^{-1}. The initial rates of product formation in the presence of PAMI inhibitor are shown in a double-reciprocal Lineweaver-Burk plot (Figure 2). The family of straight lines intersects in the second quadrant, which indicates a noncompetitive inhibition of mixed type. The secondary plots suggest an involvement of more complex kinetic features, as the slope replot is parabolic (Figure 2). Our experimental data on the kinetics of PAMI inhibition agree with the previous observation of mixed noncompetitive inhibition associated with nonstandard secondary plots, as reported for PPA inhibition by the natural inhibitors acarbose and αAI-1 [15, 16]. The inhibition constant of K_i = 2.5 μM was determined for PAMI from the slope plot, and this value compares well with an IC_{50} of 4.1 μM obtained by using dye-labeled starch as a macromolecular substrate (Table 1).

Fluorescence Binding Studies

The interaction of PPA with PAMI (comp. I) was investigated by monitoring the changes in emission intensity of intrinsic tryptophan fluorescence, as both molecules contain tryptophan residues. PAMI and PPA display emission spectra with a maximum at 350 nm. Formation of the complex was associated with the quenching of fluorescence intensity at this wavelength, as evidenced by the comparison of the spectrum of the complex with that obtained as the sum of individual spectra for PPA and PAMI (Figure 3A). The PAMI concentration was kept at least 100 times higher than the PPA concentration to achieve saturation levels for complex formation and maximum changes in fluorescence intensity. The observed quenching suggests that tryptophan residues of the PAMI and/or PPA molecule are involved in the enzyme-inhibitor interaction. In order to analyze the topology of PAMI binding to the PPA surface, the competition experiments were performed by using two natural inhibitors, αAI-1 and acarbose, for which the binding mode is well-documented by X-ray structures [5, 17] (Figure 3A). The proteinaceous inhibitor αAI-1 interacts with a large region that surrounds the substrate binding site of PPA [2]. In accord, we found that it completely displaced PAMI from its complex with PPA due to high affinity of αAI-1 (10^{-11} M order) [18]. The concentration-dependent competition effect was observed for acarbose, an oligosaccharide inhibitor with an inhibitory constant in the micromolar range, which occupies five substrate binding subsites in the PPA active site [16, 17]. The performed analysis suggests that PAMI binds to PPA inside the region covered by αAI-1 and, more precisely, at some of the substrate binding subsites occupied by the substrate analog acarbose.

Fluorescence polarization experiments were used to determine the equilibrium dissociation constant for the PAMI and PPA complex [19]. For this purpose, we synthesized two fluorescein-labeled PAMI ligands (comps. III and IV) having different attachment sites of the fluorescein moiety (Table 2). The inhibition screening experiments showed that both derivatives have similar inhibitory potency as compared to the unlabeled PAMI (comp. I) (Table 2). The labeled ligands were used in saturation binding experiments monitored by fluorescence

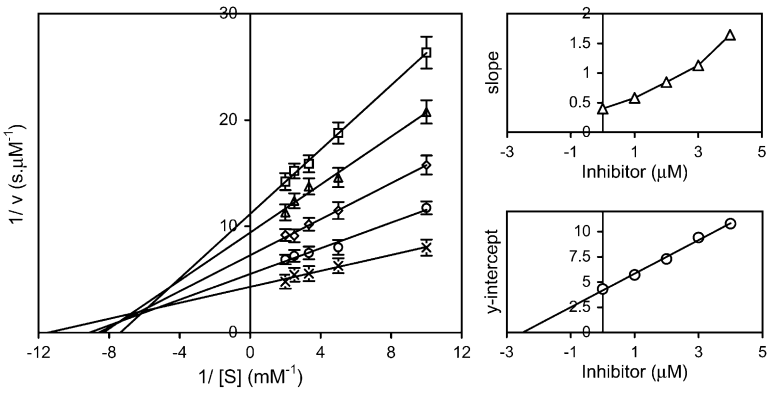

Figure 2. Kinetic Analysis of PPA Inhibition by PAMI

The Lineweaver-Burk plot for inhibition of PPA with PAMI (comp. I) is indicative of a mixed-type, noncompetitive inhibition. Activity of 1.1 nM enzyme was measured at pH 6.9 in the presence of 0–4 μM inhibitor and 0.1–0.5 mM substrate p-nitrophenyl-α-D-maltoheptaoside-4,6-O-ethylidene. The secondary plots for the same data set indicated nonstandard kinetic features with a linear y intercept replot and a parabolic slope replot. The inhibition constant of K_i = 2.5 μM was determined from the slope replot. Error bars depict ±SE of the mean of triplicates.

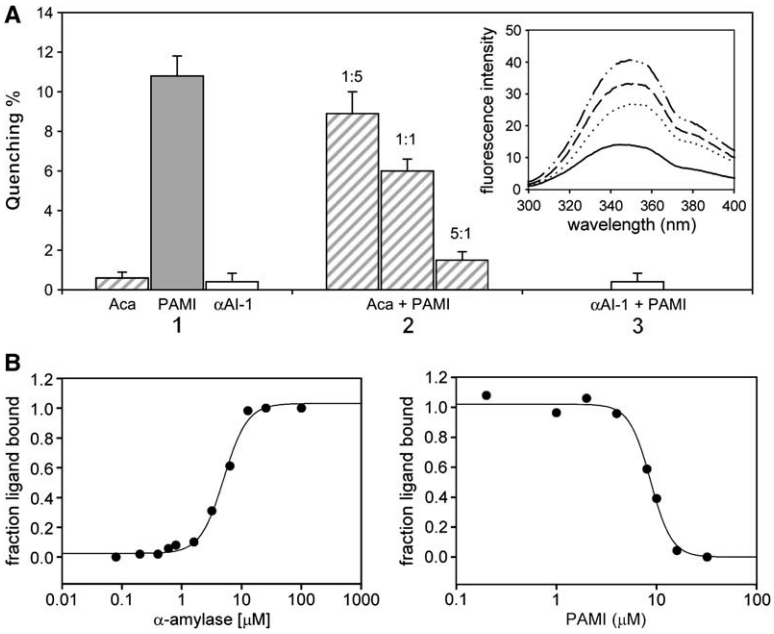

Figure 3. Fluorescence Measurements of PAMI Binding to PPA

(A) Quenching of intrinsic tryptophan fluorescence upon the formation of a complex between PAMI and PPA, and modulation of this signal by competition with natural α-amylase inhibitors acarbose (Aca) or the bean inhibitor (αAI-1). (1) Control experiments on complexation of PPA with individual inhibitors, (2) complexation of PPA with a mixture of acarbose and PAMI at the molar ratio indicated, (3) complexation of PPA with a mixture of αAI-1 and PAMI at a molar ratio of 1:100 (αAI-1:PAMI). Note that PAMI and acarbose are micromolar inhibitors and that αAI-1 is a subnanomolar inhibitor of PPA. The inset figure shows the fluorescence emission spectra of PPA (solid line), PAMI (dotted line), and the complex of PPA with PAMI (dashed line). The dashed and dotted line represents the sum of individual spectra for PPA and PAMI. The concentrations of PPA and PAMI (comp. I) were 0.3 μM and 30 μM, respectively. Error bars depict ±SE of the mean of triplicates.

(B) Fluorescence polarization assay of PAMI binding to PPA plotted as fraction of the ligand bound. Left: titration of PPA against a constant concentration of fluorescein-labeled PAMI (comp. III) (50 nM) revealed the optimized parameter K_d = 9.2 ± 0.9 μM. Right: competitive displacement of the fluorescein-labeled PAMI (10 nM) complexed with PPA (10 μM) by unlabeled PAMI (comp. I) revealed the optimized parameter K_d = 5.0 ± 0.3 μM.

anisotropy, and an analogous behavior was recorded for both compounds. Figure 3B represents a typical titration curve of PPA against the constant concentration of fluorescein-labeled PAMI for which a K_d of 9.2 μM was calculated. Further, the fluorescence polarization technique was applied in a competition assay between fluorescein-labeled and unlabeled PAMI (Figure 3B). PPA and the labeled ligand at preselected constant concentrations were incubated with various concentrations of PAMI to yield a K_d of 5.0 μM for the unlabeled ligand.

Calorimetric Analysis of Binding

The energetics of the association between PAMI and α-amylase were studied by isothermal titration calorimetry. Figure 4 shows titration of PPA with PAMI (comp. II) performed in two buffers with different ionization enthalpies. The observed enthalpy was plotted as a function of the molar ratio of PAMI to PPA, yielding the ligand to enzyme binding stoichiometry of 1.08. The binding strength of PAMI calculated from the plot corresponds to the association constant $K_A = 1.65 \times 10^5\ M^{-1}$ (K_d of 6.1 μM). The apparent reaction enthalpy measured during the reaction comprises the binding enthalpy and the enthalpy of ionization of the buffer used in the experiment. By performing identical titration experiments in two buffer systems with known ionization enthalpy, it was possible to determine an involvement of a protonation event during complex formation and to calculate the net binding enthalpy, which is buffer independent (see Experimental Procedures). This revealed that two protons (~1.83) are released during binding of PAMI to PPA. The binding enthalpy ($\Delta H_{binding}$ = −10.8 kcal/mol) and the final calculated entropy parameter ($-T\Delta S_{binding}$ = 3.7 kcal/mol) indicated that binding of PAMI to PPA is favored by enthalpic and disfavored by entropic contributions to Gibbs energy of binding ($\Delta G_{binding}$ = −7.1 kcal/mol).

Discussion

To our knowledge, we undertook for the first time the design of a low-molecular weight inhibitor of α-amylases by using a combinatorial chemistry approach. The combinatorial technique proved to provide a powerful tool for de novo creation of a structural motif complementary to the α-amylase active site cleft. The linear peptidic scaffold was chosen, as it represents a versatile template that allows for additional unnatural modifications by means of chemical synthesis and it can be applied in expression systems.

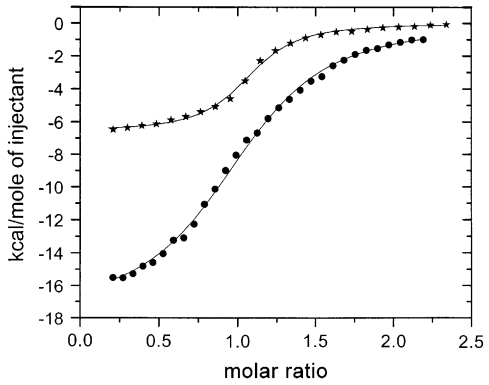

Figure 4. Isothermal Titration Calorimetry of Binding of PAMI to PPA

The heat signal was corrected for the heat of dilution and was plotted as the observed enthalpy versus the molar ratio of PAMI to PPA. The experiment was performed with 650 μM PAMI (comp. II) injected stepwise to 67 μM PPA at pH 6.9 in MES buffer (circles) and sodium cacodylate buffer (stars), respectively, at 25°C. The parameters determined: stoichiometry = 1.08 ± 0.03, K_d = 6.1 ± 0.2 μM, proton release = 1.83 ± 0.17, $\Delta H_{binding}$ = −10.8 kcal/mol ± 0.2, and $-T\Delta S_{binding}$ = 3.7 kcal/mol ± 0.2.

The discovered inhibitory motif named PAMI displays an inhibitory strength in the low micromolar range (Table 1), and it reached a submicromolar level after incorporation of a simple, unnatural substitution (IC_{50} of 0.5 μM for comp. II, Table 2). The potency of PAMI thus surpasses that of the natural oligosaccharide acarbose used in diabetes treatment [16, 20] as well as cyclic peptides developed by rational design [12, 21]. For acarbose, we measured an IC_{50} of 3.8 μM for PPA by using the same assay as for PAMI, and similar low micromolar inhibition was reported for human pancreatic and salivary α-amylases [16, 20, 22]. The cyclic peptides were derived from a β turn loop participating in the interaction of the proteinaceous α-amylase inhibitor Tendamistat with the enzyme active site [12, 21]. These β turn derivatives are about 3 orders of magnitude less potent ligands than PAMI, and this low potency clearly shows difficulties in approaching this problem by a conventional way and demonstrates an advantage of the de novo design. Tendamistat and other proteinaceous α-amylase inhibitors are nanomolar (or better) ligands whose binding strength and high degree of selectivity for α-amylases are based on the formation of an extended set of intermolecular contacts with the target enzyme. These multiple contacts are formed on a large binding interface where the macromolecular inhibitor interacts through several spatially separated segments of its folded polypeptide chain. In the case of αAI-1, the total buried area in the complex with PPA is about 3050 $Å^2$ (contributed by both molecules), one of the largest reported values for a protein-protein complex [5]. In this context, it is not surprising that the low-molecular weight inhibitor PAMI, interacting with glycoside hydrolases from family 13, displays both lower potency and broader selectivity than the proteinaceous α-amylase inhibitors. On the other hand, PAMI is more selective than the oligosaccharidic α-amylase inhibitors that are crossrecognized by several families of glycoside hydrolases [3].

To describe the PAMI interaction mode, we investigated its binding to PPA as a model α-amylase by using enzyme kinetics, fluorescence spectroscopy methods, as well as isothermal titration microcalorimetry. The magnitude of the dissociation constant in the low micromolar range determined by fluorescence study and microcalorimetry is very close to the magnitude of the inhibition constant obtained through the kinetic analysis. The intrinsic fluorescence measurements were performed to investigate PAMI binding in competition with the natural α-amylase inhibitors αAI-1 and acarbose that were previously characterized with respect to their binding mode by kinetic [15, 16] and X-ray studies [5, 17]. Our analysis clearly demonstrated that PAMI interacts with α-amylase in such a way that it occupies at least some of its substrate binding subsites. The thermodynamic characterization of PAMI revealed that its binding is favored by enthalpic and disfavored by entropic contributions to binding. The negative value determined for the binding enthalpy of PAMI is fairly low and compares well with similar values reported for other good "enthalpic inhibitors." Interestingly, these inhibitors also include low-molecular weight saccharidic inhibitors such as acarbose, tetrahydrooxazines, and iminosaccharides, whose interaction with glucoamylase and β-glucosidase was recently analyzed by microcalorimetry [23–25]. Thus, the peptidic inhibitor PAMI displays an analogous thermodynamic signature with saccharidic (i.e., substrate-like) inhibitors of glycoside hydrolases. The critical enthalpic contribution to PAMI binding suggests that a net of intermolecular interactions based on hydrogen and van der Waals bonding is formed during PAMI complexation. The analysis of ionization enthalpy showed that a transfer of two protons (from the inhibitor-enzyme complex to the bulk solution) is coupled with the binding. Hence, ionic interactions can also be involved in the formation of the complex. The origin of released protons is impossible to determine, as ionizable groups are present in the PAMI as well as the PPA binding site.

Recently published X-ray analysis of a representative collection of the complexes of proteinaceous α-amylase inhibitors showed that five structurally unrelated modes of binding to α-amylase evolved in different protein families [5–9]. We examined these structures and discovered a high content of aromatic and arginine residues at the binding interface of three nonhomologous α-amylase inhibitors. Thus, Tendamistat, αAI-1, and Amaranth inhibitors (PDB accessions 1BVN, 1DHK, and 1CLV, respectively) form about 40% of the intermolecular contacts in the respective complexes through these structural determinants (for BASI and Ragi inhibitors [1AVA and 1TMQ], this number is lower, with ~30% and 10%, respectively, of the intermolecular contacts). Such a fraction represents a significant part of the 15–40 contact residues identified to be responsible for binding of these inhibitors to α-amylases [5–7]. Importantly, arginine and aromatic residues comprise about 75% of the amino acid residues in the sequence of the PAMI peptide, and their critical importance for inhibition was demonstrated in this study with substituted derivatives of PAMI. Judging from the three-dimensional structures available, we assume that this set of key inhibitory residues reflects the composition of the complementary binding area on the α-amylase surface that is rich in acidic (including the catalytic triad Asp/Glu/Asp) and aromatic residues. Interestingly, the same inhibitory residues were recently reported to be involved in inhibition of chitinases (family 18 of glycoside hydrolases) by natural cyclopentapeptide inhibitors [26]. Taken together, the critical inhibitory determinants in the small PAMI motif are shared with those in the macromolecular proteinaceous inhibitors of α-amylases. Thus, natural molecular evolution of proteins as well as combinatorial evolution of their peptidic mimetics selected the same structural determinants, but arranged them in different spatial frameworks to establish effective interaction with the target enzyme.

The PAMI motif accomplishes the selective interaction with α-amylases in a highly effective manner by using a small peptidic scaffold with an unconstrained linear conformation. Its structure allows for various applications, including potential synthetic therapeutics or its use in expression systems to produce a recombinant peptide inhibitor or peptide fusion tag that introduces the inhibitory functionality into a carrier protein of interest. The identified PAMI motif represents a lead compound of the first generation that opens the way for further modulation of its properties by combinatorial and rational methods after determination of its exact binding

mode. The work on the X-ray structure of the PAMI-PPA complex is currently underway.

Significance

α-amylases became an important pharmacological target for treatment of diabetes as well as a plant biotechnology target for suppression of insect pests. The natural α-amylase inhibitors of protein character have attracted much attention, followed by small-molecule inhibitors of new structures and defined properties, which are now in demand. Herein, we report the first, to our knowledge, low-molecular weight inhibitory motif active against α-amylases, called PAMI, that was designed de novo through the use of combinatorial chemistry. We provide a comprehensive description of its structural requirements and interaction with the target enzymes. This analysis revealed that the small peptidic recognition motif with a simple linear scaffold represents an effective molecular mimicry of the macromolecular α-amylase inhibitors. The discovered synthetic derivatives of PAMI are more potent inhibitors of pancreatic α-amylases than the natural antidiabetic drug acarbose, and they represent promising lead compounds for therapeutic application. Further, PAMI is a good inhibitor of insect digestive α-amylases, and its synthetic gene is an attractive candidate for modification of crops to increase their resistance.

Experimental Procedures

Materials

The commercial enzymes used were α-amylases from porcine pancreas, human saliva, *B. amyloliquefaciens*, *A. oryzae* (Sigma, St.Louis, MO); *B. subtilis* and *B. licheniformis* (Fluka, Buchs, Switzerland); α-glucosidases from *S. cerevisiae* and *B. stearothermophillus* (Sigma); β-galactosidase from *E. coli* and chitinase from *S. griseus* (Fluka); cellulase from *T. viride*, β-amylase from sweet potato, and α-mannosidase from almonds (Sigma); and β-glucosidase from sweet almonds (Serva, Heidelberg, Germany). The α-glucosidases from *S. pombe* and porcine intestine were donated by P. Karasova (Institute of Chemical Technology, Praha), and porcine liver α-glucosidase was donated by I. Kluh (Institute of Organic Chemistry and Biochemistry, Praha). The activity assay substrate p-nitrophenyl-α-D-maltoheptaoside-4,6-O-ethylidene was purchased from Boehringer Manheim (Manheim, Germany), and other saccharidic substrates containing the p-nitrophenyl or 4-methylumbelliferyl groups were purchased from Sigma. Remazol Brilliant Blue-dyed starch (RBB-Starch) and OBR-hydroxyethyl-cellulose dyed with Ostazin Brilliant Red were purchased from Fluka, and Chitin azure dyed with Remazol Brilliant Violet and soluble potato starch were purchased from Sigma. The α-amylase inhibitor acarbose was purchased from Bayer (Leverkusen, Germany), and the αAI-1 inhibitor from *Phaseolus vulgaris* was purified as described previously [27]. The Fmoc precursors of L- and D-amino acids were obtained from NovaBiochem (Darmstadt, Germany), and other building blocks for peptide synthesis were obtained from Neosystem (Strasbourg, France). The D-1600 resin (Bachem, Bubendorf, Switzerland) was used for combinatorial synthesis, and Wang resin (NovaBiochem) and TentaGel S RAM resin (Rapp polymere, Tubigen, Germany) were used for conventional peptide synthesis.

Preparation of Peptides and Peptide Libraries

The primary library of soluble L-amino acid hexapeptide mixtures, Ac-B_1B_2XXXX-NH_2, was synthesized in dual-positional format. The defined position B contained one of the arrays of 20 proteinogenic amino acids, and the randomized position X contained an equimolar mixture of 20 proteinogenic amino acids. Formats for iterative L-amino acid hexa- to octapeptide libraries were Ac-$O_1O_2B_3$XXX-NH_2 to Ac-$O_1O_2O_3O_4O_5B_6$-NH_2, Ac-$O_1O_2O_3O_4O_5O_6B_7$-NH_2, and Ac-$B_8O_1O_2O_3O_4O_5O_6O_7$-NH_2, where the defined B position and the random X position is as explained above; the fixed O position contained 1 of 20 proteinogenic amino acids invariant for the particular library. Fmoc solid-phase chemistry and the split combinatorial method were used for the library synthesis [28, 29]. Peptide libraries were cleaved from solid support and were deprotected by the TFA procedure, ether extracted, and lyophilized. The peptides derived from PAMI were prepared by standard Fmoc synthetic machinery on an ABI 433A Peptide Synthesizer (Applied Biosystems, Foster City, CA) in the form of peptidyl amides containing a free or acetylated N terminus [30]. The modification of the free N terminus of GHWYYRC(tBu)WC-NH_2 with lactose derivative was performed postsynthetically with mono(lactosylamido) mono(succinimidyl)-suberate (Pierce, Rockford, IL) according to the manufacturer's protocol. The cyclization of C(Acm)GHWYYRC(tBu)WC(Acm)-NH_2 and the dimerization of GHWYYRC(Acm)WC-NH_2 was accomplished in solution by disulfide formation between S-acetamidomethyl (Acm) cysteines after their deprotection by the iodine oxidation protocol [31]. The fluorescence derivatives of GHWYYRC(tBu)WC-NH_2 and Ac-GHWYYRCWC-NH_2 were postsynthetically modified by fluorescein isothiocyanate and 5-(iodoacetamido)fluorescein (Sigma), respectively, according to the manufacturer's protocol. All PAMI derivatives were purified by reverse-phase HPLC on a Vydac C_{18} column (218TP510, Vydac, Hesperia, CA) equilibrated in 0.1% (v/v) trifluoroacetic acid at a flow rate of 3 ml/min, and they were eluted with a 1%/min gradient of 90% (v/v) acetonitrile solution in 0.1% (v/v) trifluoroacetic acid. The purified peptides were characterized by ESI mass spectrometry on a LCQ Classic Finnigan Mat (Thermo Finnigan, Bremen, Germany).

Inhibition Assays

Porcine pancreatic α-amylase (PPA) (10 pM) was preincubated for 10 min at 26°C with a peptide library (0.1–50 μg/ml) in 50 mM MES buffer (pH 6.9) containing 5 mM $CaCl_2$, 2% DMF, and 0.1 M NaCl (pH 6.9 buffer). The residual activity of PPA was determined with 0.3% (w/v) RBB-Starch as a substrate. After 20 min of incubation at 26°C, the reaction was stopped by 0.2 M NaOH, and the mixture was centrifuged. The absorbance of the supernatant was measured at 620 nm. Purified peptides in the range of 0–250 μM were used for determination of IC_{50} values. Other α-amylases were screened in the same assay: the particular enzyme concentration was set to give the same substrate conversion rate as for PPA, and the reaction mixture was buffered with 0.1 M sodium acetate buffer (pH 5.0) containing 5 mM $CaCl_2$, 2% DMF, and 50 mM NaCl. The inhibition assay of β-amylase with soluble, unlabeled potato starch (0.5%) as a substrate was performed with the neocuprine method at pH 5.5 [15]. The inhibition of cellulase from *T. viride* (at pH 5.0) and chitinase from *S. griseus* (at pH 5.5) was tested in an activity assay with the suspension substrates OBR-hydroxyethyl-cellulose (0.5%) and Chitin azure (0.1%), respectively, under a protocol recommended by the substrate manufacturer. The inhibition assay for α-glucosidases, β-glucosidase, and β-galactosidase was performed with substrates p-nitrophenyl-α-D-glucopyranoside (7 mM), p-nitrophenyl-β-D-glucopyranoside (3.5 mM), and p-nitrophenyl-β-D-galactopyranoside (0.1 mM), respectively. Generally, the enzyme (1 U/ml) was preincubated (20 min at 26°C) with peptide (0–250 μM) in 0.1 M sodium phosphate buffer (pH 6.8) containing 2% DMF (for α-glucosidases from *S. cerevisiae*, *B. stearothermophillus*, and porcine intestine) or 0.1 M sodium acetate buffer (pH 4.5) containing 2% DMF (for α-glucosidases from *S. pombe* and porcine liver) or in the latter buffer (pH 5.5) (for β-glucosidase and β-galactosidase). The kinetics of p-nitrophenol release was continuously monitored in a GENios Plus (TECAN, Salzburg, Austria) microplate reader at 405 nm. By definition, one activity unit liberates an amount of chromogenic product that gives A_{405} = 1 in 1 hr. An analogous continuous assay was used for the inhibition assay of α-mannosidase with 4-methylumbelliferyl-α-D-mannopyranoside substrate (30 μM) performed at pH 5.5 by monitoring the fluorescent product (λ_{ex} = 360 nm, λ_{em} = 465 nm). The stock solutions of peptides and peptide mixtures applied in inhibition assays were quantified by amino acid analysis on Biochrom 20 (Amersham Biosciences, Uppsala, Sweden). All measurements were performed in triplicate.

Kinetics of α-Amylase Inhibition

Determination of inhibition type was accomplished by using an activity assay with p-nitrophenyl-α-D-maltoheptaoside-4,6-O-ethylidene as a substrate [32]. A mixture of 1.1 nM PPA and 0–4 μM PAMI (comp. I) was preincubated for 10 min at 26ºC in 50 mM MES buffer (pH 6.9) containing 5 mM $CaCl_2$, 2% DMF, and 0.1 M NaCl. The reaction was started by the addition of 0.05–0.5 mM substrate and was allowed to proceed for three time intervals to determine initial velocity. The p-nitrophenol chromogen was released from digested fragments of substrate by a conversion reaction [32], and the p-nitrophenol concentration was determined from absorbance at 405 nm.

Fluorescence Measurements

The fluorescence measurements were performed with an Aminco-Bowman Series 2 Luminiscence spectrometer (Thermo Electron, Cambridge, UK). For intrinsic fluorescence analysis, an excitation wavelength of 280 nm and an emission wavelength in the range of 300–400 nm were used. The emission spectrum was recorded separately for PPA (0.3 μM), PAMI (comp. I) (30 and 150 μM), acarbose (5–150 μM), αAI-1 (0.3 μM), and their defined mixtures. The solutions were buffered by 50 mM MES buffer (pH 6.9) containing 5 mM $CaCl_2$, 5% DMF, and 0.1 M NaCl. The mixtures were incubated for 1 hr at 25ºC to allow the mixture to reach the equilibrium. As output data, the sum of PPA and individual inhibitors' emission spectra was compared with the spectrum of their mixture [33]. The percent quenching (Q) of intrinsic fluorescence was calculated by using equation:

$$Q = (1 - \frac{I_{sample}}{I_{free}})100, \quad (1)$$

where I_{free} is the sum of the fluorescence intensities of individual components before mixing, and I_{sample} is the fluorescence intensity measured for the mixture of components. The measurement performed at 350 nm giving a maximum emission signal was corroborated by the integrated signal over the range of 300–400 nm. Fluorescence polarization analysis was performed with fluorescein-labeled PAMI (comp. III or IV) at 25ºC by using excitation and emission wavelengths of 485 nm and 530 nm, respectively. Anisotropy titration was carried out with 50 nM fluorescein-labeled ligand and 0–50 μM PPA in 50 mM MES buffer (pH 6.9) containing 5 mM $CaCl_2$, 5% DMF, and 0.1 M NaCl. The mixture of the labeled ligand and PPA was incubated for 1 hr at 25ºC to reach the equilibrium. The fluorescence of the buffer alone was subtracted from each measurement, and the anisotropy was calculated according to Lakowicz [34]. G factor correction was performed by using fluorescein as a standard. The anisotropy data were converted to the fraction of the ligand bound by using equation:

$$f_b = \frac{r_{obs} - r_0}{(r_{obs} - r_0) + R(r_{max} - r_{obs})}, \quad (2)$$

where f_b is the fraction of the ligand bound and r_{obs}, r_0, and r_{max} are the observed anisotropy, anisotropy of the free ligand, and the anisotropy of the ligand bound to saturating amounts of PPA, respectively. *R* is the fluorescence intensity of the fluorophore saturated with PPA divided by the intensity of the free fluorophore. The K_d of the probe binding to PPA was determined by nonlinear least-square fit to a single-site binding model by using software Grafit (Erithacus software, Surrey, UK). Competition experiments were carried out analogously as described above with 10 μM PPA and a mixture of 50 nM fluorescein-labeled PAMI (comp. III or IV) and 0–40 μM PAMI (comp. I). The concentration of stock solutions applied was determined by amino acid analysis (PAMIs, PPA) and elementary analysis (acarbose).

Titration Microcalorimetry

Binding of PAMI (comp. II) to PPA was monitored in a VP-ITC titration microcalorimeter (Microcal, Inc., Northampton, MA) at 25ºC. The solutions of reactants were prepared in 25 mM MES (or sodium cacodylate) (pH 6.9) containing 5 mM $CaCl_2$ and 5% DMF, and their concentrations were determined by amino acid analysis. Aliquots (9 μl) of 650 μM PAMI were stepwise injected into a sample cell containing 1.43 ml of 67 μM PPA until complete saturation. Each experiment was accompanied by the corresponding control experiment in which PAMI was injected into buffer alone. The heat due to the binding reaction between the inhibitor and the enzyme was obtained as the difference between the measured heat of the reaction and the corresponding heat of the dilution determined in the control experiment [35]. The thermodynamic parameters, stoichiometry, and K_A values were calculated by ORIGIN 5.0 sofware (Microcal, Inc.). A proton transfer between the binding complex and the buffer molecules was evaluated by performing the titration experiments in two buffers with different ionization enthalpies (3.72 kcal/mol for the MES buffer, −0.47 kcal/mol for the cacodylate buffer) [36]. The calculation of parameters Δn and $\Delta H_{binding}$ was performed essentially as described previously [37] according to:

$$\Delta H_{ITC} = \Delta H_{binding} + \Delta n \Delta H_{ion}, \quad (3)$$

where Δn is the number of transferred protons upon binding, $\Delta H_{binding}$ is the buffer-independent binding enthalpy, ΔH_{ion} is the ionization enthalpy of buffer, and H_{ITC} is the apparent enthalpy.

Acknowledgments

We would like to thank M. Kožíšek for his expertise in microcalorimetry; P. Karasová, I. Kluh, and I. Pražáková for help with screening of selected α-glucosidases; M. Pravcová for screening of selected α-amylases; I. Bláha, M. Hradilek, M. Machová, J. Velek, and M. Blechová for assistance with peptide synthesis; J. Cvačka and J. Kohoutová for mass spectrometry; J. Zbrožek and V. Himrová for amino acid analysis; and L. Rulíšek and M. Baudyš for fruitful discussions. This work was supported by the Grant Agency of the Czech Republic (Grant No. 203/02/P081), the European Cooperation in the field of Scientific and Technical Research D16 Action (Ministry of Education, Youth and Sports of the Czech Republic, Project No. OCD16.001), and by the research project Z40550506.

Received: March 18, 2005
Revised: September 14, 2005
Accepted: October 11, 2005
Published: December 16, 2005

References

1. Breuer, H.W. (2003). Review of acarbose therapeutic strategies in the long-term treatment and in the prevention of type 2 diabetes. Int. J. Clin. Pharmacol. Ther. *41*, 421–440.
2. Franco, O.L., Rigden, D.J., Melo, F.R., and Grossi-De-Sa, M.F. (2002). Plant α-amylase inhibitors and their interaction with insect α-amylases. Eur. J. Biochem. *269*, 397–412.
3. Truscheit, E., Frommer, W., Junge, B., Müller, L., Schmidt, D.D., and Wingender, W. (1981). Chemistry and biochemistry of microbial α-glucosidase inhibitors. Angew. Chem. Int. *20*, 744–761.
4. Svensson, B., Fukuda, K., Nielsen, P.K., and Bonsager, B.C. (2004). Proteinaceous α-amylase inhibitors. Biochim. Biophys. Acta *1696*, 145–156.
5. Bompard-Gilles, C., Rousseau, P., Rouge, P., and Payan, F. (1996). Substrate mimicry in the active center of a mammalian α-amylase: structural analysis of an enzyme-inhibitor complex. Structure *4*, 1441–1452.
6. Wiegand, G., Epp, O., and Huber, R. (1995). The crystal structure of porcine pancreatic α-amylase in complex with the microbial inhibitor Tendamistat. J. Mol. Biol. *247*, 99–110.
7. Pereira, P.J., Lozanov, V., Patthy, A., Huber, R., Bode, W., Pongor, S., and Strobl, S. (1999). Specific inhibition of insect α-amylases: yellow meal worm α-amylase in complex with the amaranth α-amylase inhibitor at 2.0 Å resolution. Structure *7*, 1079–1088.
8. Vallee, F., Kadziola, A., Bourne, Y., Juy, M., Rodenburg, K.W., Svensson, B., and Haser, R. (1998). Barley α-amylase bound to its endogenous protein inhibitor BASI: crystal structure of the complex at 1.9 Å resolution. Structure *6*, 649–659.
9. Strobl, S., Maskos, K., Wiegand, G., Huber, R., Gomis-Ruth, F.X., and Glockshuber, R. (1998). A novel strategy for inhibition of α-amylases: yellow meal worm α-amylase in complex with the Ragi bifunctional inhibitor at 2.5 Å resolution. Structure *6*, 911–921.

10. Lehtio, J., Teeri, T.T., and Nygren, P.A. (2000). α-amylase inhibitors selected from a combinatorial library of a cellulose binding domain scaffold. Proteins *41*, 316–322.
11. Desmyter, A., Spinelli, S., Payan, F., Lauwereys, M., Wyns, L., Muyldermans, S., and Cambillau, C. (2002). Three camelid VHH domains in complex with porcine pancreatic α-amylase. Inhibition and versatility of binding topology. J. Biol. Chem. *277*, 23645–23650.
12. Matter, H., and Kessler, H. (1995). Structures, dynamics, and biological activities of 15 cyclic hexapeptide analogs of the α-amylase inhibitor Tendamistat (HOE 467) in solution. J. Am. Chem. Soc. *117*, 3347–3359.
13. Baumann, H., Ohrman, S., Shinohara, Y., Ersoy, O., Choudhury, D., Axen, A., Tedebark, U., and Carredano, E. (2003). Rational design, synthesis, and verification of affinity ligands to a protein surface cleft. Protein Sci. *12*, 784–793.
14. Coutinho, P.M., and Henrissat, B. (1999). Carbohydrate-Active Enzymes Server at URL (http://afmb.cnrs-mrs.fr/CAZY/).
15. Koukiekolo, R., Le Berre-Anton, V., Desseaux, V., Moreau, Y., Rouge, P., Marchis-Mouren, G., and Santimone, M. (1999). Mechanism of porcine pancreatic α-amylase inhibition of amylose and maltopentaose hydrolysis by kidney bean (*Phaseolus vulgaris*) inhibitor and comparison with that by acarbose. Eur. J. Biochem. *265*, 20–26.
16. Al Kazaz, M., Desseaux, V., Marchis-Mouren, G., Prodanov, E., and Santimone, M. (1998). The mechanism of porcine pancreatic α-amylase. Inhibition of maltopentaose hydrolysis by acarbose, maltose and maltotriose. Eur. J. Biochem. *252*, 100–107.
17. Qian, M., Haser, R., Buisson, G., Duee, E., and Payan, F. (1994). The active center of a mammalian α-amylase. Structure of the complex of a pancreatic α-amylase with a carbohydrate inhibitor refined to 2.2-Å resolution. Biochemistry *33*, 6284–6294.
18. Powers, J.R., and Whitaker, J.R. (1977). Effect of several experimental parameters on combination of red kidney bean (*Phaseolus vulgaris*) α-amylase inhibitor with porcine pancreatic α-amylase. J. Food Biochem. *1*, 239–260.
19. Roehrl, M.H., Wang, J.Y., and Wagner, G. (2004). A general framework for development and data analysis of competitive high-throughput screens for small-molecule inhibitors of protein-protein interactions by fluorescence polarization. Biochemistry *43*, 16056–16066.
20. Ferey-Roux, G., Perrier, J., Forest, E., Marchis-Mouren, G., Puigserver, A., and Santimone, M. (1998). The human pancreatic α-amylase isoforms: isolation, structural studies and kinetics of inhibition by acarbose. Biochim. Biophys. Acta *1388*, 10–20.
21. Sefler, A.M., Kozlowski, M.C., Guo, T., and Bartlett, P.A. (1997). Design, synthesis, and evaluation of a depsipeptide mimic of tendamistat. J. Org. Chem. *62*, 93–102.
22. Kandra, L., Zajacz, A., Remenyik, J., and Gyemant, G. (2005). Kinetic investigation of a new inhibitor for human salivary α-amylase. Biochem. Biophys. Res. Commun. *334*, 824–828.
23. Gloster, T.M., Macdonald, J.M., Tarling, C.A., Stick, R.V., Withers, S.G., and Davies, G.J. (2004). Structural, thermodynamic, and kinetic analyses of tetrahydrooxazine-derived inhibitors bound to β-glucosidases. J. Biol. Chem. *279*, 49236–49242.
24. Zechel, D.L., Boraston, A.B., Gloster, T., Boraston, C.M., Macdonald, J.M., Tilbrook, D.M., Stick, R.V., and Davies, G.J. (2003). Iminosugar glycosidase inhibitors: structural and thermodynamic dissection of the binding of isofagomine and 1-deoxynojirimycin to β-glucosidases. J. Am. Chem. Soc. *125*, 14313–14323.
25. Solovicova, A., Christensen, T., Hostinova, E., Gasperik, J., Sevcik, J., and Svensson, B. (1999). Structure-function relationships in glucoamylases encoded by variant *Saccharomycopsis fibuligera* genes. Eur. J. Biochem. *264*, 756–764.
26. Houston, D.R., Shiomi, K., Arai, N., Omura, S., Peter, M.G., Turberg, A., Synstad, B., Eijsink, V.G., and van Aalten, D.M. (2002). High-resolution structures of a chitinase complexed with natural product cyclopentapeptide inhibitors: mimicry of carbohydrate substrate. Proc. Natl. Acad. Sci. USA *99*, 9127–9132.
27. Kluh, I., Horn, M., Hyblova, J., Hubert, J., Doleckova-Maresova, L., Voburka, Z., Kudlikova, I., Kocourek, F., and Mares, M. (2005). Inhibitory specificity and insecticidal selectivity of α-amylase inhibitor from *Phaseolus vulgaris*. Phytochemistry *66*, 31–39.
28. Eichler, J., and Houghten, R.A. (1993). Identification of substrate-analog trypsin inhibitors through the screening of synthetic peptide combinatorial libraries. Biochemistry *32*, 11035–11041.
29. Pinilla, C., Appel, J., Blondelle, S., Dooley, C., Dorner, B., Eichler, J., Ostresh, J., and Houghten, R.A. (1995). A review of the utility of soluble peptide combinatorial libraries. Biopolymers *37*, 221–240.
30. Atherton, E., and Sheppard, R.C. (1989). Solid Phase Peptide Synthesis: A Practical Approach (Oxford, UK: IRL Press at Oxford University Press).
31. Kamber, B., Hartmann, A., Eisler, K., Riniker, B., Rink, H., Sieber, P., and Rittel, W. (1980). The synthesis of cystine peptides by iodine oxidation of S-trityl-cysteine and S-acetamidomethyl-cysteine peptides. Hevl. Chim. Acta *63*, 899–915.
32. Rauscher, E., Neumann, U., Schaich, E., von Bulow, S., and Wahlefeld, A.W. (1985). Optimized conditions for determining activity concentration of α-amylase in serum, with 1,4-α-D-4-nitrophenylmaltoheptaoside as substrate. Clin. Chem. *31*, 14–19.
33. Horn, M., Pavlik, M., Doleckova, L., Baudys, M., and Mares, M. (2000). Arginine-based structures are specific inhibitors of cathepsin C. Application of peptide combinatorial libraries. Eur. J. Biochem. *267*, 3330–3336.
34. Lakowicz, J.R. (1999). Principles of Fluorescence Spectroscopy (New York: Plenum).
35. Pierce, M.M., Raman, C.S., and Nall, B.T. (1999). Isothermal titration calorimetry of protein-protein interactions. Methods *19*, 213–221.
36. Fukada, H., and Takahashi, K. (1998). Enthalpy and heat capacity changes for the proton dissociation of various buffer components in 0.1 M potassium chloride. Proteins *33*, 159–166.
37. Raffa, R.B., Stagliano, G.W., and Spencer, S.D. (2004). Protonation effect on drug affinity. Eur. J. Pharmacol. *483*, 323–324.